THE ASTROPHYSICAL JOURNAL, 572:L131–L134, 2002 June 20

COSMIC SHEAR AND POWER SPECTRUM NORMALIZATION WITH THE *HUBBLE SPACE TELESCOPE*

ALEXANDRE REFREGIER,[1] JASON RHODES,[2,3] AND EDWARD J. GROTH[4]

Received 2002 March 8; accepted 2002 May 8; published 2002 May 24

ABSTRACT

Weak lensing by large-scale structure provides a direct measurement of matter fluctuations in the universe. We report a measurement of this "cosmic shear" based on 271 Wide Field Planetary Camera 2 archival images from the *Hubble Space Telescope* Medium Deep Survey. Our measurement method and treatment of systematic effects were discussed in an earlier paper. We measure the shear variance on scales ranging from 0.′7 to 1.′4, with a detection significance greater than 3.8 σ. This allows us to measure the normalization of the matter power spectrum to be $\sigma_8 = (0.94 \pm 0.10 \pm 0.14)(0.3/\Omega_m)^{0.44}(0.21/\Gamma)^{0.15}$, in a ΛCDM universe. The first 1 σ error includes statistical errors only, while the latter also includes (Gaussian) cosmic variance and the uncertainty in the galaxy redshift distribution. Our results are consistent with earlier cosmic shear measurements from the ground and from space. We compare our cosmic shear results and those from other groups to the normalization from cluster abundance and galaxy surveys. We find that the combination of four recent cosmic shear measurements are somewhat inconsistent with the recent normalization using these methods and discuss possible explanations for the discrepancy.

Subject headings: dark matter — gravitational lensing — large-scale structure of universe — methods: data analysis

On-line material: color figures

1. INTRODUCTION

Weak gravitational lensing by large-scale structure has been shown to be a valuable method of measuring mass fluctuations in the universe (see Mellier at al. 2001 for a review). This effect has been detected both from the ground (Wittman et al. 2000; Van Waerbeke et al. 2000, 2001; Bacon, Refregier, & Ellis 2000; Bacon et al. 2002; Kaiser, Wilson, & Luppino 2000; Hoekstra et al. 2002) and from space (Rhodes, Refregier, & Groth 2001, hereafter RRGII; Hämmerle et al. 2001). These results bode well for the prospect of measuring cosmological parameters and the mass distribution of the universe using weak lensing.

In this Letter, we present the highest significance detection of cosmic shear using space-based images. It is based on images from the *Hubble Space Telescope* (*HST*) Medium Deep Survey (MDS; Ratnatunga, Griffiths, & Ostrander 1999). We apply the methods for the correction of systematic effects and detection of shear we have previously developed (Rhodes, Refregier, & Groth 2000, hereafter RRGI) to 271 Wide Field Planetary Camera 2 (WFPC2) fields in the MDS. The method of RRGI is specifically adapted to *HST* images and takes advantage of the small point-spread function (PSF) of the *HST* (0.″1 as compared to ∼0.″8 from the ground). This affords us a higher surface density of resolved galaxies as well as a diminished sensitivity to PSF smearing when compared to ground-based measurements. We develop an optimal depth-weighted average of selected MDS fields to extract a weak-lensing signal. We then use this signal to derive constraints on the amplitude of the mass power spectrum and compare this to measurements from previous cosmic shear surveys and from other methods.

[1] Institute of Astronomy, Madingley Road, Cambridge CB3 OHA, UK; ar@ast.cam.ac.uk.

[2] Laboratory for Astronomy and Solar Physics, Goddard Space Flight Center, Code 681, Greenbelt, MD 20771; jrhodes@band1.gsfc.nasa.gov.

[3] NASA/National Research Council Research Associate.

[4] Department of Physics, Princeton University, Jadwin Hall, P.O. Box 708, Princeton, NJ 08544; groth@pupgg.princeton.edu.

2. DATA

The MDS consists of primary and parallel observations taken with the WFPC2 on *HST*. We selected only the *I*-band images in chips 2, 3, and 4 to study weak lensing. To ensure random lines of sight, we discarded fields that were pointed at galaxy clusters, leaving us with 468 *I*-band fields. To ensure that our fields are independent, we selected 291 fields separated by at least 10′, beyond which scale the lensing signal drops considerably (see Fig. 2).

We used the MDS object catalogs (Ratnatunga et al. 1999) to determine the position, magnitude, and area of each object, as well as to separate galaxies from stars. We used the chip-specific backgrounds listed in the MDS SKYSIG files, which are consistent with backgrounds calculated using the IRAF task IMARITH. Not using object-specific backgrounds necessitated the discarding of another 20 fields with a large sky gradient. Our final catalog thus consisted of 271 WFPC2 fields amounting to an area of about 0.36 deg^2.

3. PROCEDURE

The procedure we used for measuring galaxy ellipticities and shear from the source images is described in detail in RRGI (see also RRGII and Rhodes 1999). It is based on the method introduced by Kaiser, Squires, & Broadhurst (1995), but modified and tested for applications to *HST* images. The usefulness of our method was demonstrated by our detection of cosmic shear in the *HST* Groth Strip (RRGII).

We correct for camera distortion and convolution by the anisotropic PSF using Gaussian-weighted moments. Camera distortions were corrected using a map derived from stellar astrometric shifts (Holtzman et al. 1995). PSF corrections were determined from *HST* observations of four stellar fields These fields were chosen to span the focus range of the *HST* as shown by Biretta et al. (2000). Finally, we derive the ellipticities ϵ_i of the galaxies and convert them into shear estimates using $\gamma_i = G^{-1}\epsilon_i$, where G is the shear susceptibility factor given by equation (30) in RRGI.

To limit the impact of noise and systematics, we made a number of cuts to select our galaxy sample. We first discarded objects for which $\epsilon > 4$ after deconvolution. To avoid using galaxies with low signal-to-noise ratio, we included only galaxies that have a magnitude $I < (I'_m + 2)$, where I'_m is the median magnitude (before the cut) of the field and chip in which the galaxy lies. This is consistent with the magnitude cut we made in RRGII. We also discarded small galaxies (size $d < 1.5$ pixels) in order to minimize the effects of the anisotropic PSF on our measurements (see RRGI). The final galaxy sample contained about 3.1×10^4 galaxies. The distribution of the median magnitude I_m (after the cuts) of our fields is shown in Figure 1, which reveals a wide range of depth for the MDS.

For the magnitude range of the MDS ($19 < I < 27$), we use spectroscopic redshift determinations from the DEEP survey (DEEP Collaboration 1999, private communication) and the Hubble Deep Fields (Lanzetta, Yahil, & Fernández-Soto 1996[5]) to determine that the median redshift z_m in a field is related to the median magnitude I_m by the equation

$$z_m \simeq 0.722 + 0.149(I_m - 22.0). \quad (1)$$

This agrees well with an extrapolation of the Canada-France Redshift Survey redshift distribution (Lilly et al. 1995) we used to determine the median redshift of objects in the Groth Strip (RRGII). Both methods give $z_m = 0.9 \pm 0.1$ for the Groth Strip ($I_m = 23.6$), where the error gives a measure of the 1 σ systematic uncertainty in the above relation.

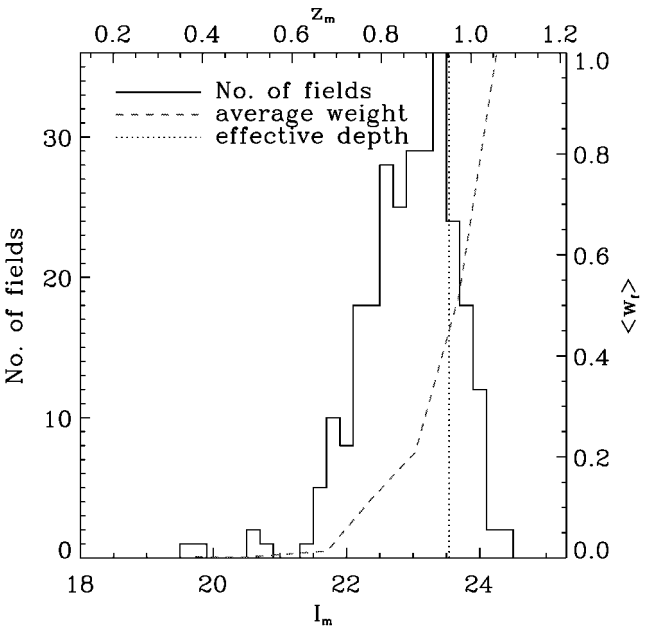

FIG. 1.—Distribution of the median magnitudes I_m of the fields (*solid line and left y-axis*). The top *x*-axis shows the approximate corresponding median redshift according to eq. (1). The weights of the fields $\langle w_f \rangle$ averaged in each magnitude bin are shown as the dashed line and right *y*-axis, in arbitrary units. The effective depth of the survey with this weighted scheme is shown as the vertical dotted line and corresponds to $I_m = 23.5$ or $z_m = 0.95 \pm 0.10$. [*See the electronic edition of the Journal for a color version of this figure.*]

4. ESTIMATOR FOR THE SHEAR VARIANCE

We wish to derive a measure of the shear variance on different angular scales by averaging over the $N_c = 3$ chips in each of the $N_f = 271$ fields. As explained in § 3, the fields have varying depths but are sufficiently far apart to be statistically independent. As in RRGII, the total mean shear γ_{icf} in chip c and field f can be measured by averaging over all the selected galaxies that it contains. It is equal to the sum of contributions from lensing, from noise, and from systematics, and can thus be written as $\gamma_{icf} = \gamma_{icf}^{\rm lens} + \gamma_{icf}^{\rm noise} + \gamma_{icf}^{\rm sys}$. The noise variance $\sigma^2_{{\rm noise},\,cf} \equiv \langle |\gamma_{cf}^{\rm noise}|^2 \rangle$ can be measured from the data by computing the error in the mean γ_{icf} from the distribution of the galaxy shears inside the chip. As RRGI showed, the systematics are greatly reduced if the shear is averaged over the chip scale and if small galaxies (with $d < 0\farcs15$) are discarded. In this case, the systematics are dominated by the time variations of the PSF and induce a shear variance $\sigma^2_{{\rm sys},\,cf} \equiv \langle |\gamma_{cf}^{\rm sys}|^2 \rangle$ approximately equal to 0.0011^2 (see RRGII).

For each field f, an estimator for the shear variance $\sigma^2_{\rm lens}$ on the chip scale is given by

$$\hat{\sigma}^2_{{\rm lens},\,f} = \frac{1}{N_c} \sum_c |\gamma_{cf}|^2 - \sigma^2_{{\rm noise},\,f} - \sigma^2_{{\rm sys},\,f}, \quad (2)$$

where $\sigma^2_{{\rm noise},\,f} = N_c^{-1} \sum_c \sigma^2_{{\rm noise},\,cf}$, and similarly for $\sigma^2_{{\rm sys},\,f}$. Assuming Gaussian statistics, the error variance of the combined estimator is given by (see Bacon et al. 2000 for the case $N_c = 2$)

$$\sigma^2(\hat{\sigma}^2_{{\rm lens},\,f}) \simeq \frac{1}{N_c} (\sigma^2_{{\rm lens},\,f} + \sigma^2_{{\rm noise},\,f} + \sigma^2_{{\rm sys},\,f})^2 + \frac{2}{N_c^2} \sum_{c \neq c'} \sigma^2_{\times\, cc'f}, \quad (3)$$

where $\sigma^2_{\times\, cc'f} = \langle \gamma^{\rm lens}_{1cf} \gamma^{\rm lens}_{1c'f} \rangle + \langle \gamma^{\rm lens}_{2cf} \gamma^{\rm lens}_{2c'f} \rangle$ is the cross-correlation between chips c and c' and can also be measured from the data. The term $\sigma^2_{{\rm lens},\,f}$ corresponds to cosmic variance, and the last term arises because the chips within a field are not statistically independent. While the lensing shear field is known to be non-Gaussian on scales smaller than about $10'$ (e.g., Jain & Seljak 1997), the non-Gaussian corrections to this error estimate are small for noise-dominated two-point statistics like the variance (see discussion in RRGII and White & Hu 2000).

Because the fields have a range of depths, it is desirable to combine the individual estimators $\hat{\sigma}^2_{{\rm lens},\,f}$ using a weighting scheme of the form

$$\hat{\sigma}^2_{\rm lens} = \sum_f w_f \hat{\sigma}^2_{{\rm lens},\,f} \Big/ \sum_f w_f. \quad (4)$$

A convenient choice for the weights is given by

$$w_f = \sigma^{-4}_{{\rm noise},\,f}, \quad (5)$$

i.e., to the inverse square of the noise contribution to the error in $\hat{\sigma}^2_{{\rm lens},\,f}$. This weighting scheme is nearly optimal and avoids including the lensing signal $\sigma^2_{{\rm lens},\,f}$ itself. The average weights $\langle w_f \rangle$ in several magnitude bins are shown in Figure 1. As expected, deeper fields have larger weights since they contain a larger number of galaxies and thus have a smaller value of $\sigma_{{\rm noise},\,f}$.

To measure the shear variance on the field scale, we first average the shear within each field and apply the same procedure. This time, however, the cross-correlation term in equation (3) vanishes since each field is independent. Similarly, we can consider pairs of chips to measure the shear variance on intermediate scales.

[5] See also http://www.ess.sunysb.edu/astro for data.

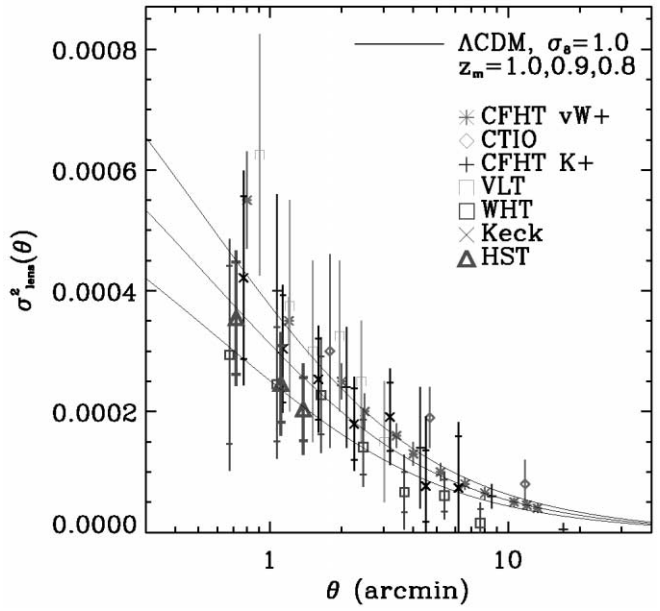

FIG. 2.—Shear variance $\sigma^2_{\rm lens}$ as a function of the radius θ of a circular cell, including our observed value (*HST*) as well as that observed by other groups: Van Waerbeke et al. (2001; CFHT vW+), Wittman et al. (2000; CTIO), Kaiser et al. (2000; CFHT K+), Maoli et al. (2001; VLT), Bacon et al. (2002; WHT and Keck). For our measurement, the inner error bars correspond to noise only, while the outer error bars correspond to the total error (noise+cosmic variance). The errors for the measurements of Maoli et al. (2001) and Van Waerbeke et al. (2001) do not include cosmic variance. The measurements of Hämmerle et al. (2001) and Hoekstra et al. (2002) are not displayed but are consistent with the other measurements. Also displayed are the predictions for a ΛCDM model with $\Omega_m = 0.3$, $\sigma_8 = 1$, and $\Gamma = 0.21$. The galaxy median redshift was taken to be $z_m = 1.0$, 0.9, and 0.8, from top to bottom, respectively. [*See the electronic edition of the Journal for a color version of this figure*.]

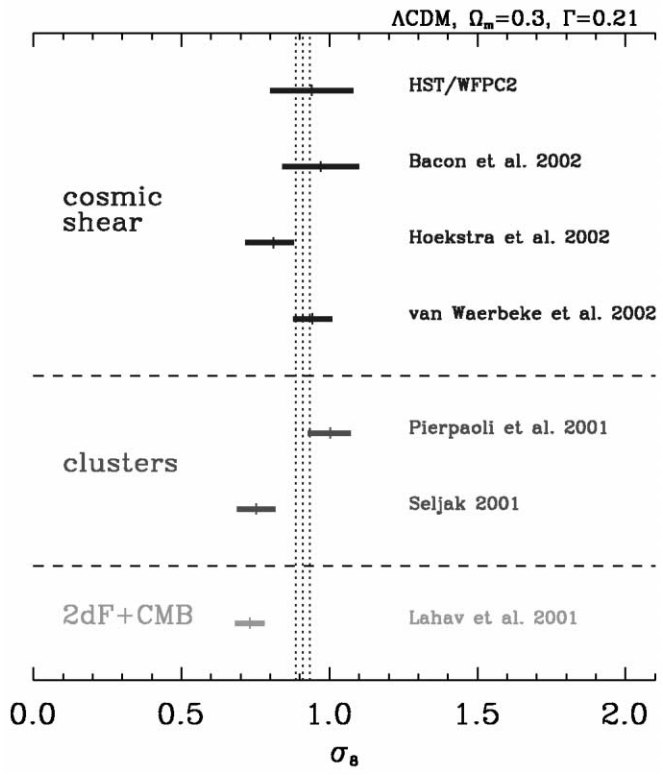

FIG. 3.—Comparison of the determination of σ_8 by different groups and methods. The errors have all been converted to 1 σ, and a ΛCDM model with $\Omega_m = 0.3$ and $\Gamma = 0.21$ was assumed (except for Van Waerbeke et al. 2002, who marginalized over Γ between 0.1 and 0.4). The vertical dotted lines show the weighted average (weights proportional to σ^{-2}) of the four cosmic shear measurements and associated 1 σ error. [*See the electronic edition of the Journal for a color version of this figure*.]

5. RESULTS

Our measurement for the shear variance $\sigma^2_{\rm lens}(\theta)$ on different scales is shown in Figure 2. The angular scale θ is the radius of an effective circular cell whose mean pair separation equals that of the chip configuration considered ($\theta \simeq 0\farcm72$, $1\farcm11$, and $1\farcm38$, for 1, 2, and 3 $1\farcm27$ chips, respectively). The outer 1 σ error bars include both statistical errors and cosmic variance (from eq. [3]), while the inner error bars only include statistical errors (i.e., by setting $\sigma^2_{\rm lens}$ and $\sigma^2_\times$ to 0 on the right-hand side of this equation). For instance, on the chip scale we obtain $\sigma^2_{\rm lens}(0\farcm72) = (3.5 \pm 0.9 \pm 1.1) \times 10^{-4}$, yielding a detection significance (inner error) of 3.8 σ with this scale alone. As a check of systematics, we analyzed our signal into *E*- and *B*-modes using the aperture mass $M_{\rm ap}(0\farcm67)$ statistic on the chip scale (Schneider et al. 1998; Van Waerbeke et al. 2001). For *E*-modes, we find the upper limit $\langle M^2_{{\rm ap},E}\rangle = (0.4 \pm 1.7) \times 10^{-4}$ (1 σ), which is consistent with the signal expected in a Λ cold dark matter (ΛCDM) model ($\langle M^2_{{\rm ap},E}\rangle \simeq 0.6 \times 10^{-4}$; Schneider et al. 1998). For the *B*-modes, we find $\langle M^2_{{\rm ap},B}\rangle = (0.3 \pm 1.7) \times 10^{-4}$ (1 σ), as expected in the absence of systematics (which corresponds to $\langle M^2_{{\rm ap},B}\rangle \equiv 0$).

The measurements from other groups are also plotted in Figure 2, along with the predictions for a ΛCDM model with $\sigma_8 = 1$ and $\Gamma = 0.21$. The central value for Γ is close to the recent measurement of this parameter from galaxy clustering (e.g., Percival et al. 2001), while keeping the $\Gamma = \Omega_m h$ relation valid for $h = 0.7$. The predictions are plotted for a range of galaxy redshifts $z_m = 0.9 \pm 0.1$, corresponding approximately to the uncertainty and dispersion of this parameter in the different surveys. In our case, the effective median *I* magnitude of our measurement is $I_m = \sum_f w_f I_{m,f} / \sum_f w_f \simeq 23.5$, which corresponds to a median redshift of $z_m = 0.95 \pm 0.10$ (see eq. [1]). The effective magnitude and corresponding redshift are plotted in Figure 1. Given the range of median redshifts in the different surveys and the correlation between angular bins for the variance, our results are in good agreement with these other measurements and with the ΛCDM model.

Our measurements can be used to constrain cosmological parameters. Because our measurements on different scales are not independent, we conservatively only consider the shear variance on the chip scale ($\theta = 0\farcm72$). Within a ΛCDM model, it is predicted to be (see RRGII), within an excellent approximation,

$$\sigma_{\rm lens} \simeq 0.0202 \left(\frac{\sigma_8}{1}\right)^{1.27} \left(\frac{\Omega_m}{0.3}\right)^{0.56} \left(\frac{z_m}{0.95}\right)^{0.89} \left(\frac{\Gamma}{0.21}\right)^{0.19}, \quad (6)$$

where σ_8 is the amplitude of mass fluctuations on $8\,h^{-1}$ Mpc scales and Ω_m is the matter density parameter. Inverting this equation, we find that our measurement of $\sigma^2_{\rm lens}$ yields $\sigma_8 = (0.94 \pm 0.10 \pm 0.12)(\Omega_m/0.3)^{-0.44}(\Gamma/0.21)^{-0.15}(z_m/0.95)^{-0.70}$, where the first error is statistical only and the second also includes cosmic variance. To this error must be added that arising from the uncertainty in the median effective redshift $z_m = 0.95 \pm 0.10$. After propagating this error, we obtain

$$\sigma_8 = (0.94 \pm 0.10 \pm 0.14) \left(\frac{0.3}{\Omega_m}\right)^{0.44} \left(\frac{0.21}{\Gamma}\right)^{0.15}, \quad (7)$$

where the first error reflects statistical errors only, and the latter is the total error and includes statistical errors, cosmic variance, and redshift uncertainty (all 1 σ).

Figure 3 shows the comparison of our measurement of σ_8 (*HST*/WFC2) with that from other weak-lensing surveys and from other methods. A ΛCDM model with $\Omega_m = 0.3$ and $\Gamma = 0.21$ was assumed (except for Van Waerbeke et al. 2001, who marginalized over Γ). Our σ_8-value is consistent with the other recent cosmic shear measurements of Bacon et al. (2002), Hoekstra et al. (2002), and Van Waerbeke et al. (2002) and also with the "old" normalization from cluster abundance (e.g., Pierpaoli, Scott, & White 2001). This was recently revised to a lower normalization, by using the observed mass-temperature relation rather than that derived from numerical simulations (e.g., Seljak 2001). A similar normalization was derived by combining measurements of galaxy clustering from Two Degree Field and cosmic microwave background anisotropy (Lahav et al. 2001). Our results are consistent with this new normalization at the 1.4 σ level.

6. DISCUSSION AND CONCLUSION

We have achieved the highest significance detection of cosmic shear using space-based images to date. Using the MDS, we have detected the shear variance on 0.′7 to 1.′4 scales with a significance greater than 3.8 σ. From the amplitude of the signal we derived a normalization of the matter power spectrum given by equation (7), with errors that include statistical errors, (Gaussian) cosmic variance, and the uncertainty in the galaxy redshift distribution. Our results agree with previous measurements of the rms shear using both ground- and space-based images at the 1 σ level and with the "old" (e.g., Pierpaoli et al. 2001) and "new" (e.g., Seljak 2001) cluster abundance normalization at the 0.4 σ and 1.4 σ level, respectively.

A weighted average of the four recent cosmic shear measurements shown in Figure 3 yields $\sigma_8 = 0.91 \pm 0.02$, for a ΛCDM model with $\Omega_m = 0.3$ and $\Gamma = 0.21$ (see vertical bars in Fig. 3). This is consistent with the old cluster normalization at the 1.2 σ level but somewhat inconsistent with the new cluster normalization at the 2.5 σ level, where the uncertainty is dominated by that from cluster abundance. This discrepancy could be caused by unknown systematics in the cluster abundance or cosmic shear methods. For the latter case, the calibration of the shear measurement methods would need to be revisited, in the context of current and upcoming surveys. The inaccuracy of the calculation of the nonlinear power spectrum and of the halo mass function may also contribute to the error budget. If confirmed, however, this discrepancy could have important consequences for our understanding of the physics of clusters or may require extensions of the standard ΛCDM paradigm for structure formation.

We thank David Bacon, Richard Massey, and Richard Ellis for fruitful discussions and the anonymous referee for useful suggestions. A. R. was supported by an EEC fellowship from the TMR network on Gravitational Lensing and by a Wolfson College Research Fellowship. E. J. G. was supported by NASA grant NAG5-6279. J. R. was supported by a National Research Council–GSFC Research Associateship. The Medium Deep Survey catalog is based on observations with the NASA/ESA *Hubble Space Telescope*, obtained at the Space Telescope Science Institute, which is operated by the Association of Universities for Research in Astronomy.

REFERENCES

Bacon, D. J., Massey, R., Refregier, A., & Ellis, R. 2002, MNRAS, submitted (astro-ph/0203134)
Bacon, D. J., Refregier, A., & Ellis, R. S. 2000, MNRAS, 318, 625
Biretta, J. A., et al. 2000, WFPC2 Instrument Handbook, Version 5.0 (Baltimore: STScI)
Hämmerle, H., et al. 2001, A&A, 385, 743
Hoekstra, H., et al. 2002, ApJ, in press (astro-ph/0202285)
Holtzman, J., et al. 1995, PASP, 107, 1065
Jain, B., & Seljak, U. 1997, ApJ, 484, 560
Kaiser, N., Squires, G., & Broadhurst, T. 1995, ApJ, 449, 460
Kaiser, N., Wilson, G., & Luppino, G. A. 2000, ApJL, submitted (astro-ph/0003338)
Lahav, O., et al. 2001, MNRAS, submitted (astro-ph/0112162)
Lanzetta, K., Yahil, A., & Fernández-Soto, A. 1996, Nature, 381, 759
Lilly, S., et al. 1995, ApJ, 455, 108
Maoli, R., et al. 2001, A&A, 368, 766
Mellier, Y., et al. 2001, in Deep Fields, Proc. ESO/ECF/STScI Workshop, ed. S. Cristiani, A. Renzini, & R. E. Williams (Berlin: Springer)
Percival, W., et al. 2001, MNRAS, 327, 1297
Pierpaoli, E., Scott, D., & White, M. 2001, MNRAS, 325, 77
Ratnatunga, K., Griffiths, R., & Ostrander, E. 1999, AJ, 118, 86
Rhodes, J. 1999, Ph.D. thesis, Princeton Univ.
Rhodes, J., Refregier, A., & Groth, E. J. 2000, ApJ, 536, 79 (RRGI)
———. 2001, ApJ, 552, L85 (RRGII)
Schneider, P., Van Waerbeke, L., Jain, B., & Kruse, G. 1998, MNRAS, 296, 873
Seljak, U. 2001, MNRAS, submitted (astro-ph/0111362)
Van Waerbeke, L., et al. 2000, A&A, 358, 30
———. 2001, A&A, 374, 757
———. 2002, A&A, submitted (astro-ph/0202503)
White, M., & Hu, W. 2000, ApJ, 537, 1
Wittman, D. M., Tyson, J. A., Kirkman, D., Dell'Antonio, I., & Bernstein, G. 2000, Nature, 405, 143